The impact of slope positions on stand transpiration of a *Zenia insignis* plantation in North Guangdong Province, South China

Huixia Li*, Hongyi Zhou*, Xinghu Wei, Zhaoxiong Liang, Shujuan Liu, Jinguo Huang

Department of Resources and Environment, Foshan University, Foshan 528000, China, emails: 316019683@qq.com (H. Li), 27450277@qq.com (H. Zhou)

ABSTRACT

Understanding the impact of slope positions on stand transpiration of a plantation is necessary for assessing the hydrological effect of the plantation and furtherly, quantifying the watershed water budget. In this study, we analyzed the variations in hourly, daily, and monthly stand transpiration of a 25 y old *Zenia insignis* plantation at different slope positions, and its response to climate factors, soil water content, and leaf area index in a karst catchment of north Guangdong province, south China. Results showed that all plots for different slope positions exhibit the same sequence sorted by hourly, daily, and monthly stand sap flux density (J_s), which is upper-slope, foot-slope, and mid-slope in descending order. Meanwhile, all plots for different slope positions exhibit the same sequence sorted by hourly, daily, and monthly stand-scale transpiration (E), which is foot-slope, upper-slope, and mid-slope in descending order. Hourly J_s values are positively correlated with solar radiation (R_s), air temperature (T_a), vapor pressure deficit (VPD) ($p < 0.001$), and negatively correlated with relative humidity (RH) ($p < 0.001$). Daily J_s values are positively correlated with R_s, T_a, VPD ($p < 0.001$). Monthly J_s is mainly affected by LAI. Generally, there is no significant correlation between J_s and soil moisture at all hourly, daily, and monthly scale, but there is a strong positive relation between hourly J_s and soil moisture in moist days. The findings of this study will assist in evaluating local water budgets in *Z. insignis* dominated karst catchments of South China.

Keywords: Stand-scale transpiration; *Zenia insignis*; Karst catchment; South China

1. Introduction

Transpiration, as a significant component of the water budget and hydrothermal process, has a considerable impact on regional water resources and is related to ecosystem productivity, species distribution, and ecosystem sustainability [1–4]. In karst mountain ecosystems, temporary drought caused by the special geological structure will result in disharmony among water, soil, and vegetation systems [5], and furtherly threaten ecosystem health and ecological security. Previous studies have improved our knowledge about plant transpiration in karst ecosystems at both leaf scale and individual scale [6–8]. Nonetheless, few studies have examined spatial variations in stand transpiration in karst mountain regions [3]. Therefore, it's an urgent task to understand variations in and controls of plant water use at stand scale in karst ecosystems.

Rocky desertification is the most serious eco-environmental problems in karst mountain regions [9]. *Zenia insignis* is one of the most important species for rocky desertification control. It has played a significant role in vegetation restoration in karst mountain regions of southwestern China. However, general knowledge about the long-term adaptability of *Z. insignis* plantation to fragile karst environment is still unavailable. Huang et al. [6] reported *Z. insignis* has good eco-physiological adaption

---

* Corresponding author.

to dry and hot karst environment and is an excellent pioneer plant for karst rocky desertification control. While some literature showed that cultivation of *Z. insignis* was not an effective method for soil productivity improvement and ecosystem restoration [10,11]. Clearly, more studies are needed to rigorously examine the variations in transpiration of *Z. insignis* to accurately evaluate the sustainability of *Z. insignis* plantation in karst environment.

As an important factor influencing spatial heterogeneity in ecological ecosystems, topographic gradients cause variations in ecological process and plant growth patterns along a slope by reallocating the heat, water, and nutrient [3,12] and, accordingly, significant spatial variations in tree transpiration [13,14]. Previous studies have revealed the relationship between transpiration and topography at a leaf scale using eddy covariance technique [15], and also at a regional scale using remote sensing technique [16–18]. Yet the responses of stand transpiration to different slope positions and the variations in controlling factors are still poorly understood. Therefore, this study made an attempt to include topographic factors to properly describe plant transpiration at a stand scale, which is important for the accurate evaluation of catchment or landscape scale transpiration.

Thus, understanding the variations in transpiration of *Z. insignis* with different slope positions in karst ecosystems is important not only for regional water budgets, but also for karst rocky desertification control, and sustainable management of plantation. To provide scientific basis for modifying water balance equation in karst areas, this study aimed to clarify variations in stand transpiration at different slope positions of a karst hill covered with *Z. insignis*, one of the most important plantation species for rocky desertification control in karst ecosystems.

2. Materials and methods

2.1. Study area description

This study was conducted in a 25-year-old *Z. insignis* plantation (24°26′N, 112°43′E) located in the north of Guangdong, China. It is an eco-demonstration region for rocky desertification control with an area of 7.06 km². The altitude ranges from 50 to 250 m and the slope varies from 5° to 60°. The average annual temperature was 20.8°C in 2016, with maximum and minimum monthly temperature of approximately 28.7°C in July and 11.0°C in January, respectively. The annual rainfall was 2,022 m in 2016 and was unevenly distributed with about 76% occurred during March to September.

2.2. Sample plots and sample trees

We installed three sample plots along a slope in a *Z. insignis* plantation enclosed for afforestation without any management practices after planting. The three plots are on the same slope of a typical karst hill with similar rock bareness (>80%; Table 1). The slope degrees of the plots for upper, middle, and lower-slope positions are about 46°, 33°, and 7°, respectively. The area of each plot is 10 × 10 m². We selected three sample trees in each plot and measured their height, diameter at breast height (DBH; cm; i.e., 1.3 m

aboveground), and leaf area index (LAI; m²/m²). We also calculated their sapwood depth (T_s; cm) and sapwood area (A_s; cm²) using a regression equation between DBH and A_s to avoid injuring sample trees.

All the mean height, mean DBH, mean T_s, mean A_s, LAI of sample trees increased from up-slope to down-slope (Table 1). The mean height was 7.50, 8.50, and 10.73 m, the mean DBH was 14.67, 15.17, and 20.37 cm, the mean T_s was 0.81, 0.84, and 1.12 cm, the mean A_s was 37.45, 39.99, and 66.56 cm², the average LAI was 2.63, 2.89, and 3.07, respectively, for upper, middle, and lower-slope plots.

2.3. Sapwood determination

Sapwood is the most important water-conducting tissue of trees [19], so A_s is closely related to sap flow and transpiration. We selected 24 sample trees beside the sample plots and took an increment core at breast height for each sample tree. We estimated the bulk thickness (T_b; cm), T_s, and heartwood thicknesses (T_h; cm) visually in the field by different color and then confirmed in the lab by soaking the core in 0.005% ferric chloride solution to make the sapwood boundary more easily visible [20]. The relationship between DBH and A_s was determined using a power regression [21] and the equation is expressed as Eq. (1):

$$A_s = 0.3897DBH^{1.6997} \tag{1}$$

2.4. Sap flow measurement

The thermal dissipation probes (TDP) were used to determine F_d for *Z. insignis* trees at each plot. A TDP sensor consists of two needles with 10 mm in length and 1.2 mm in diameter. Heated upper needle temperature is compared to lower ambient temperature needle. The temperature difference between two needles was measured every 30 s

Table 1
Characteristics of the study plot and sample trees for sap flow measurement

Characteristics	Upper-slope	Mid-slope	Foot-slope
Sample number	3	3	3
Rock coverage (%)	>80	>80	>80
Elevation (m)	120.1	101.7	72.5
Slope degree (°)	46	33	7
Age (a)	25	25	25
Mean height (m)	7.5	8.5	10.73
Mean DBH (cm)	14.67	15.17	20.37
Mean T_s (cm)	0.81	0.84	1.12
Mean A_s (cm²)	37.45	39.99	66.56
LAI (m²/m²)	2.63	2.89	3.07

Note: DBH, diameter at breast height; T_s, sapwood depth; A_s, sapwood area; LAI, leaf area index. LAI was derived from the average monthly values from May to October during the growing season of 2016. Mean T_s and mean A_s were measured at breast height of the stem (1.3 m aboveground).

and recorded the mean value every 10 min in a CR10XTD data logger (Campbell Scientific Inc., Logan, UT, USA). Maximum temperature difference occurs when sap flow rate is zero, and it decreases with the increase of sap flow [22].

F_d (g/m² s) was calculated using the empirical equation based on temperature difference between the two needles developed by Granier [23]:

$$F_d = 86.4 \times 119 \times \left(\frac{\Delta T_m - \Delta T}{\Delta T} \right)^{1.231} \tag{2}$$

where ΔT (°C) is the temperature difference between the heated needle and the reference needle, and ΔT_m (°C) is the maximum temperature difference at zero sap flow usually occurring at night.

If the needle length is longer than T_s, ΔT was calibrated according to the study of Clearwater et al. [24]:

$$\Delta T_{sw} = \Delta T - \frac{b\Delta T_m}{a} \tag{3}$$

where ΔT_{sw} (°C) is the temperature difference in the sapwood; a is the proportion of needle in the sapwood; and b is the proportion of needle in the inactive xylem ($b = 1 - a$).

2.5. Stand-scale E estimates

We scaled up individual tree measurements to stand scale using the following equation [25,26]:

$$E = \frac{J_s A_{ST}}{A_G} \tag{4}$$

where E (kg/d) is the stand-scale transpiration, J_s (kg/m² d) is stand sap flux density computed as the area weighted mean F_d of all sample trees in a plot [26,27], A_{ST} (m²) is total sapwood area in study plot and A_G (m²) is the ground area.

2.6. Meteorology and soil moisture

Solar radiation (R_s), relative humidity (RH), and air temperature (T_a) were monitored at intervals of 10 min using weather sensors (AV-20P, AV-10TH, AVALON, USA) in the experimental field. Precipitation (P) data were obtained from China meteorological data service center (http://data.cma.cn). Vapor pressure deficit (VPD) was calculated from air temperature and relative humidity [28–30]:

$$es\left(T_a\right) = 0.611 \times \exp\left(\frac{17.502 T_a}{T_a + 240.97} \right) \tag{5}$$

$$VPD = es\left(T_a\right) - \frac{es \times RH}{100} \tag{6}$$

where es(T_a) is saturated water vapor pressure (kPa), T_a is air temperature (°C), and RH is relative humidity (%).

Soil water content (SWC) data for the top 20 cm soil layer was monitored for each plot using soil moisture probes (AV-EC5, AVALON, USA) and recorded at intervals of 10 min in a CR10XTD data logger (Campbell Scientific Inc., Logan, UT, USA).

3. Results

3.1. Climate and soil water conditions

The variations in climate variables and SWC over the study period were shown in Fig. 1. Daily R_s ranged from 21.7 to 366.4 Wm⁻², with the average of 161.3 ± 83.7 W/m². Daily T ranged from 3.7°C to 31.1°C, with the average of 20.8°C ± 7.0°C. Daily RH ranged from 53.8% to 100%, with the average of 87.9% ± 9.0%. Daily VPD ranged from 0.00 to
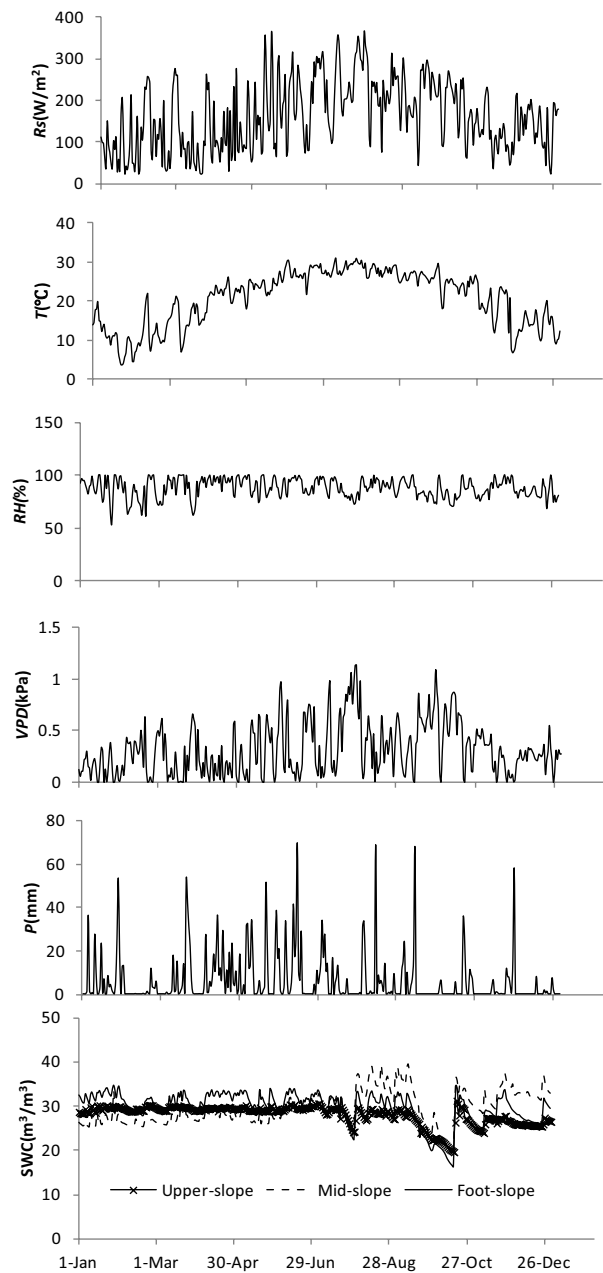
Fig. 1. Variations in climate variables and soil water content over the study period.

1.13 kPa, with the average of 0.31 ± 0.26 kPa. The total precipitation of the year was 2,080 mm, with the maximum of 326 mm occurring in June. Mean daily SWC of three sample plots varied in a similar pattern over the study period, with a valley value occurring in early and middle October.

3.2. Hourly J_s, E, and influence factors

For the three plots at different slope positions, hourly J_s and E on three randomly selected sunny days (16th September to 18th September) in growing season showed a similar pattern over the course of a day. Transpiration began at about 7:00–8:00 in the morning, increased quickly, and reached the maximum value during 11:00–14:00, dropped sharply at 17:00–18:00, then decreased slowly after 19:00, and approached zero at midnight (Fig. 2). Hourly J_s of *Z. insignis* plantation was highest at the upper-slope and lowest at the mid-slope. However, hourly E was higher at foot-slope than at upper-slope. Hourly J_s is positively correlated with R_s, T_a, and VPD ($p < 0.001$), and negatively correlated with RH ($p < 0.001$), but not significantly correlated with SWC (Table 2), which indicates that the transpiration of *Z. insignis* is greatly influenced by meteorological factors at hourly scale.

3.3. Daily J_s, E, and influence factors

The average daily J_s in growing season was, in descending order, 1,232.73 kg/m² d for upper-slope plot,

1,049.10 kg/m² d for foot-slope plot, and 621.40 kg/m² d for mid-slope plot. The average daily E in growing season was, in descending order, 1.57 kg/d for foot-slope plot, 0.85 kg/d for upper-slope plot, and 0.52 kg/d for mid-slope plot. The date on which peak J_s occurred was different for different slope position plot (Fig. 3). It occurred in June on the upper-slope, in July on the foot-slope, and in August on the middle-slope. Daily J_s is positively correlated with R_s, T_a, and VPD ($p < 0.001$), but not significantly correlated with RH, P, and SWC (Table 3).

3.4. Monthly E and influence factors

The average monthly E was, in descending order, 32.28 kg/month for foot-slope plot, 18.20 kg/month for upper-slope plot, and 13.55 kg/month for mid-slope plot. Calculated by different seasons (Fig. 4), the average monthly E for all plots was, in descending order, 31.35 kg/month in summer, 19.02 kg/month in autumn, 13.37 kg/month in spring, and 11.53 kg/month in winter. Mean E during vigorous growth season of *Z. insignis* (May to October) accounted for 71% of the whole year. At monthly scale, LAI is the only factor significantly correlated ($p < 0.001$) to sap flux density for all plots on different slope position (Table 4). For upper-slope plot, sap flux density is also greatly influenced by R_s. For foot–slope plot, sap flux density is also significantly correlated to R_s, T_a, and VPD.

4. Discussion

4.1. Variations in J_s and E on different slope positions

Our data showed that J_s values are various on different slope positions. All at hourly, daily, and monthly scales, the sequence sorted by J_s in descending order is upper-slope, foot-slope, and mid-slope. This result was in consistent with the study conducted in a karst *Platycladus orientalis* forest in China [31], while it was in contrast to the results derived in a Japanese cedar forest by Kumagai at al. [32] which showed J_s values were similar in the up-slope plot and low-slope plot in the growing season. Meanwhile, Kume et al. [3] found J_s values in up-slope plot were lower those in low slop plot in a Japanese cypress plantation. All these studies were conducted in a homogenous plantation, but the species and stand structure such as tree age, height, and DBH were different, which might cause the variations
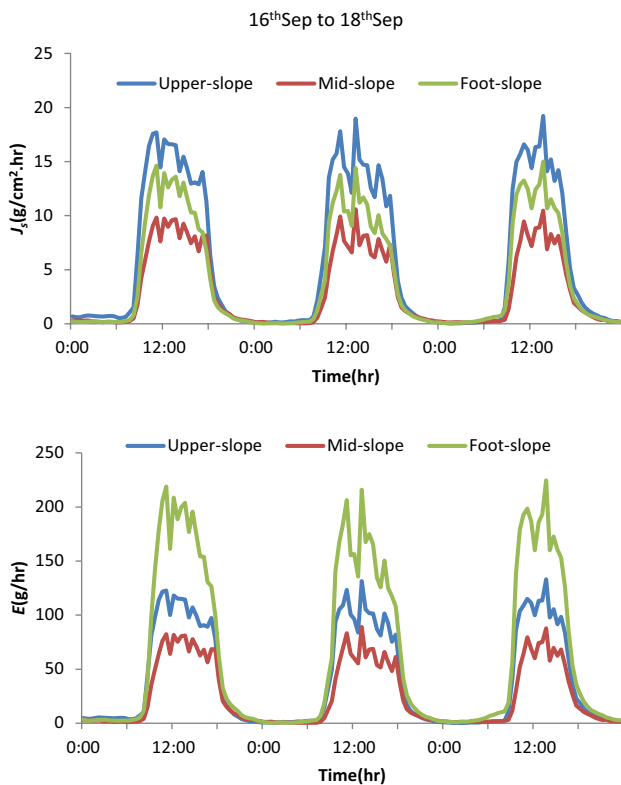
Fig. 2. Variations in hourly stand sap flux density and hourly stand-scale transpiration of the sample plots on upper-slope, middle-slope, and foot-slope, respectively.

Table 2
Correlation coefficients between hourly J_s and R_s, T_a, RH, VPD, and SWC

Factors	Upper-slope	Mid-slope	Foot-slope
R_s (W/m²)	0.8741[a]	0.8807[a]	0.8879[a]
T_a (°C)	0.8505[a]	0.8841[a]	0.8338[a]
RH (%)	−0.8486[a]	−0.8871[a]	−0.8355[a]
VPD (kPa)	0.8512[a]	0.8922[a]	0.8380[a]
SWC (m³/m³)	0.1036	0.0822	0.0859

Note: n = 366. [a]indicates significant at 0.001 level. J_s, stand sap flux densities; R_s, solar radiation; T_a, air temperature; RH, relative humidity; VPD, vapor pressure deficit; SWC, soil water content.
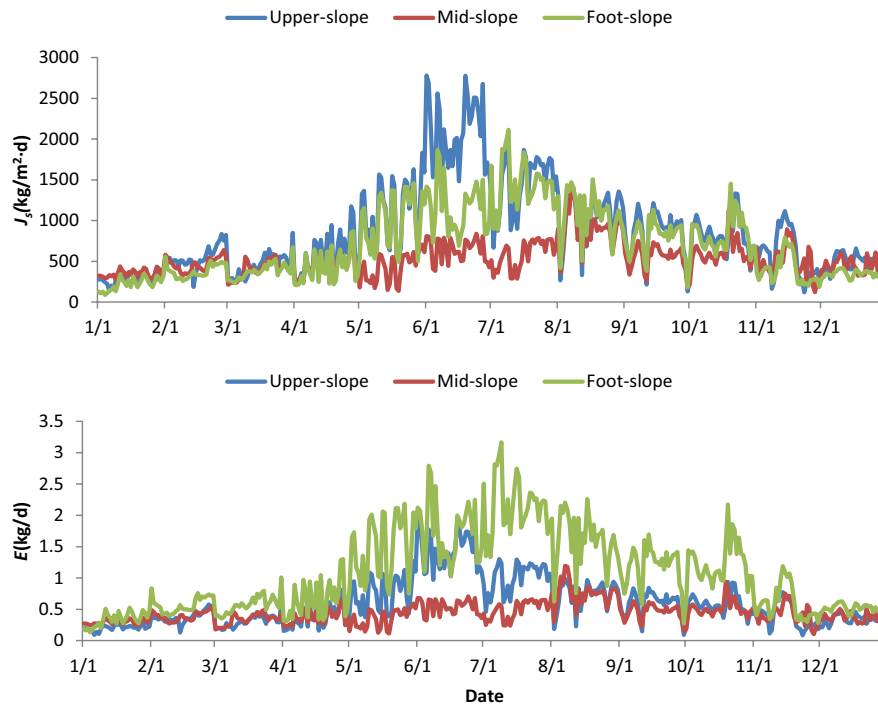
Fig. 3. Variations in daily stand sap flux density and hourly stand-scale transpiration of the sample plots on upper-slope, middle-slope, and foot-slope, respectively.

Table 3
Correlation coefficients between daily J_s and R_s, T_a, RH, VPD, P, and SWC

Factors	Upper-slope	Mid-slope	Foot-slope
R_s (W/m^2)	0.6388[a]	0.44508[a]	0.6698[a]
T_a (°C)	0.69418[a]	0.3888[a]	0.7706[a]
RH (%)	−0.1094	−0.1613	−0.0921
VPD (kPa)	0.5270[a]	0.4278[a]	0.5520[a]
P (mm)	−0.0815	−0.1118	−0.0682
SWC (m^3/m^3)	0.0435	0.0132	0.0055

Note: n = 366. [a]indicates significant at 0.001 level. J_s, stand sap flux densities; R_s, solar radiation; T_a, air temperature; RH, relative humidity; VPD, vapor pressure deficit; P, precipitation; SWC, soil water content.

Fig. 4. Average monthly stand-scale transpiration of all sample plots in different seasons.

Table 4
Correlation coefficients between monthly J_s and R_s, T_a, RH, VPD, P, SWC, and LAI

Factors	Upper-slope	Mid-slope	Foot-slope
R_s (W/m^2)	0.8319[a]	0.7241	0.9512[a]
T_a (°C)	0.778	0.678	0.8972[a]
RH (%)	0.235	0.1091	0.1628
VPD (kPa)	0.6264	0.5754	0.8141[a]
P (mm)	0.3613	−0.0096	0.2962
SWC (m^3/m^3)	0.16658	0.629	−0.0651
LAI	0.835[a]	0.8124[a]	0.9023[a]

Note: n = 12. [a]indicates significant at 0.001 level. J_s, stand sap flux densities; R_s, solar radiation; T_a, air temperature; RH, relative humidity; VPD, vapor pressure deficit; P, precipitation; SWC, soil water content; LAI, leaf area index.

in J_s among these studies. In addition, it was reported that R_s, which is significant positively related to J_s, was higher on upper-slope than that on lower-slope [33–35].

Different from J_s, the sequence sorted by E in descending order, at all hourly, daily, and monthly scales, is foot-slope, upper-slope, and mid-slope, which is mainly caused by the differences both in sapwood area and J_s among the three plots (Table 1, Fig. 5). Kume et al. [3] showed the similar results derived in a Japanese cypress plantation, while Kumagai et al. [32] and Ford et al. [36] reported the differences in E between upper-slope and lower-slope was mainly caused by sapwood area. Thus, the main causes of the variations in E for different slope position cannot be simply generalized. It depends on the scales of spatial

variations both in sapwood area and J_s. Comparing the relationship between J_s and E in upper-slope and foot-slope, the regression trend line in foot-slope is above the 1:1 line while that in upper-slope is under the 1:1 line (Fig. 5), indicating that E values in foot-slope increased more quickly with J_s values than in upper-slope. This could be explained by the bigger sapwood area in foot-slope than that in upper-slope.

4.2. Influence factors for J_s on different slope positions

Our data showed that hourly J_s values are positively correlated with R_s, T_a, and VPD ($p < 0.001$), and negatively correlated with RH ($p < 0.001$). In upper-slope and foot-slope plots, hourly J_s values are most strongly related to R_s, while in mid-slope plot, hourly J_s values are most strongly related to VPD. Daily J_s values are also positively correlated with R_s, T_a, and VPD ($p < 0.001$), and they are also most strongly related to R_s in upper-slope and foot-slope plots, while most strongly related to T_a in mid-slope plot. Monthly J_s values are positively related with LAI ($p < 0.001$) in all plots on different slope position. In upper-slope plot, monthly J_s is also greatly influenced by R_s. In foot-slope plot, monthly J_s are also significantly correlated to R_s, T_a, and VPD. On the whole, hourly and daily J_s is mainly controlled by climate factors, and monthly J_s is mainly affected by LAI. This result was in consistent with our study about the influence factors for J_s of Z. insignis under different rock bareness rate [20], and it was also in accordance with the results derived in a black locust plantation on the semi-arid Loess Plateau of China [37].

Our data also showed that there is no significant correlation between J_s and soil moisture at all hourly, daily, and monthly scale (Table 5). This may partly due to the thin and discontinuous soil layer in karst ecosystems [20], and just as Huang et al. [8] and Jackson et al. [38] reported, deep roots of rock plants can extract water from stable source such as epikarst water and cave streams. However, the data during moist days (RH = 100%) showed a strong positive relation between hourly J_s and soil moisture for all plots of different slope positions (Table 5) [39–41]. The possible reason may be the phenomenon of plant water spitting caused by root pressure.

4.3. Limitations

The main limitation of our research was the limited dataset. An entire dataset for a longer period of time could lead to a higher generalization of our results. Although we have continuously measured J_s for 3 y, the datasets for 2017 and 2018 are incomplete due to some broken probes. However, from the results of the limited dataset for 1 y, we could also find a clear pattern which exhibits the correlation between stand transpiration and slope positions.

5. Conclusions

This study aimed to reveal the relationship between slope positions and stand transpiration of a Z. insignis plantation in southern China and to analyze the influence factors at different temporal scales. The sequence
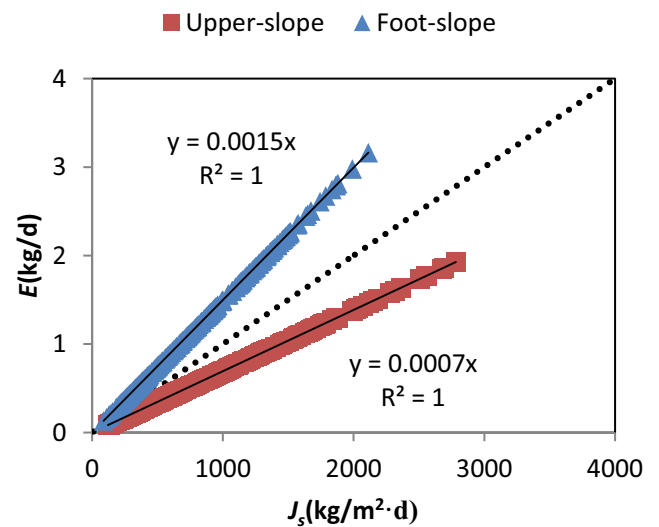
Fig. 5. Comparison between the mean sap flux density (J_s) and the stand transpiration (E) in the upper-slope (UP) and foot-slope (LP) in 2016. The 1:1 line is represented by a dotted line. The black lines represent linear regressions ($p < 0.001$ for all linear regressions).

Table 5
Correlation coefficients between hourly J_s and SWC under moist weather conditions from 19th to 20th May

Factors	Upper-slope	Mid-slope	Foot-slope
R_s (W/m^2)	−0.0757	−0.0386	−0.1165
T_a (°C)	0.1799	0.1195	0.1101
RH (%)	−0.0343	−0.0531	−0.0375
VPD (kPa)	0.0343	0.0531	0.0375
SWC (m^3/m^3)	−0.8056[a]	−0.9374[a]	−0.8496[a]

Note: $n = 288$. [a]indicates significant at 0.001 level. J_s, stand sap flux densities; SWC, soil water content.

sorted by J_s in descending order is upper-slope, foot-slope, and mid-slope all at hourly, daily, and monthly scales. The sequence sorted by E in descending order is foot-slope, upper-slope, and mid-slope at all hourly, daily, and monthly scales. Hourly J_s values are positively correlated with R_s, T_a, and VPD ($p < 0.001$), and negatively correlated with RH ($p < 0.001$). Daily J_s values are positively correlated with R_s, T_a, and VPD ($p < 0.001$). Monthly J_s is mainly affected by LAI. Generally, there is no significant correlation between J_s and soil moisture at all hourly, daily, and monthly scale, but there is a strong positive relation between hourly J_s and soil moisture in moist days.

References

[1] K.B. Wilson, P.J. Hanson, P.J. Mulholland, D.D. Baldocchi, S.D. Wullschleger, A comparison of methods for determining forest evapotranspiration and its components: sap-flow, soil water budget, eddy covariance and catchment water balance, Agric. For. Meteorol., 106 (2001) 153–168.

[2] L. Christensen, C.L. Tague, J.S. Baron, Spatial patterns of simulated transpiration response to climate variability in a snow dominated mountain ecosystem, Hydrol. Process, 22 (2008) 3576–3588.

[3] T. Kume, K. Tsuruta, H. Komatsu, Y. Shinohara, A. Katayama, Differences in sap flux-based stand transpiration between upper and lower slope positions in a Japanese cypress plantation watershed, Ecohydrology, 9 (2016) 1105–1116.

[4] A. Tian, Y. Wang, A.A. Webb, Z. Liu, P.T. Yu, W. Xiong, X. Wang, Partitioning the causes of spatiotemporal variation in the sunny day sap flux density of a larch plantation on a hillslope in northwest China, J. Hydrol., 571 (2019) 503–515.

[5] S.Y. He, J.C. Ran, D.X. Yuan, Y.Q. Xie, A comparative study on hydrological and ecological effects in different karst ecosystems, Acta Geosci. Sin., 3 (2001) 265–270.

[6] Y.Q. Huang, X.Y. Wang, S.H. Lu, Q. Wang, P. Zhao, Studies of photosynthesis, transpiration and water use efficiency of some dominant species in rocky desert area, Guangxi, China, Guihaia, 2 (2006) 171–177.

[7] W. Li, G. Wu, L.J. Yu, Y. Liu, K. Xia, M.T. Li, Comparative studies on transpiration characteristics of vitex negundo at different geomorphological positions at Guilin karst experimental site, Plant Sci. J., 3 (2007) 316–319.

[8] Y.Q. Huang, X.K. Li, Z.F. Zhang, C.X. He, P. Zhao, Y.M. You, L. Mo, Seasonal changes in *Cyclobalanopsis glauca* transpiration and canopy stomatal conductance and their dependence on subterranean water and climatic factors in rocky karst terrain, J. Hydrol., 402 (2011) 135–143.

[9] S.J. Wang, The most serious geologically environmental problem in southwestern China— karst rocky desertification, Bull. Mineral. Petrol. Geochem., 2 (2003) 120–126.

[10] T.Q. Song, W.X. Peng, F.P. Zeng, K.L. Wang, L. Liu, S.Y. Lu, H. Du, Soil ecological effects of converting cropland to forest and grassland in depressions between karst hills, Acta Pedol. Sin., 6 (2011) 1219–1226.

[11] W.X. Peng, T.Q. Song, F.P. Zeng, K.L. Wang, H. Du, S.Y. Lu, Models of vegetation and soil coupling coordinative degree in grain for green project in depressions between karst hills, Trans. CSAE, 9 (2011) 305–310.

[12] F.J. Swanson, T.K. Kratz, N. Caine, R.G. Woodmansee, Landform effects on ecosystem patterns and processes, Bioscience, 38 (1988) 82–98.

[13] C. Van der Tol, A.J. Dolman, M.J. Waterloo, K. Raspor, Topography induced spatial variations in diurnal cycles of assimilation and latent heat of Mediterranean forest, Biogeosciences, 4 (2007) 137–154.

[14] I.A.M. Yunusa, C.D. Aumann, M.A. Rabb, N. Merrick, P.D. Fisher, P.L. Eberbach, D. Eamus, Topographical and seasonal trends in transpiration by two co-occurring Eucalyptus species during two contrasting years in a low rainfall environment, Agric. For. Meteorol., 150 (2010) 1234–1244.

[15] C.J. Shan, Z.S. Liang, R.L. Han, W.F. Hao, Characteristics of *Robinia pseudoacacia* water physiological ecology under different habitats in north Shaanxi gully areas of loess plateau, J. Appl. Ecol., 7 (2005) 1205–1212.

[16] M. Elmaayar, J. Chen, Spatial scaling of evapotranspiration as affected by heterogeneities in vegetation, topography, and soil texture, Remote Sens. Environ., 102 (2006) 33–51.

[17] H.K. Kafle, Y. Yamaguchi, Effects of topography on the spatial distribution of evapotranspiration over a complex terrain using two-source energy balance model with ASTER data, Hydrol. Processes, 16 (2009) 2295–2306.

[18] L. Liang, L. Li, Q. Liu, Spatial distribution of reference evapotranspiration considering topography in the Taoer river basin of northeast China, Hydrol. Res., 5 (2010) 424–437.

[19] X.P. Peng, J. Fan, Q.J. Wang, D. Warrington, Discrepancy of sap flow in *Salix matsudana* grown under different soil textures in the water-wind erosion crisscross region on the Loess Plateau, Plant Soil, 390 (2015) 383–399.

[20] H.X. Li, H.Y. Zhou, X.H. Wei, N. Lu, Z.X. Liang, Variations in sap flow of *Zenia insignis* under different rock bareness rate in north Guangdong, China, J. Mountain Sci., 16 (2019) 2320–2334.

[21] R.A. Vertessy, R.G. Benyon, S.K. O'Sullivan, P.R. Gribben, Relationships between stem diameter, sapwood area, leaf area and transpiration in a young mountain ash forest, Tree Physiol., 9 (1995) 559–567.

[22] A. Granier, Une nouvelle methode pour la mesure du flux de seve brute dans le trone des arbres, Ann. Sci. For., 42 (1985) 193–200.

[23] A. Granier, Evaluation of transpiration in a Douglas-fir stand by means of sap flow measurements, Tree Physiol., 3 (1987) 309–320.

[24] M.J. Clearwater, F.C. Meinzer, J.L. Andrade, G. Goldstein, N.M. Holbrook, Potential errors in measurement of nonuniform sap flow using heat dissipation probes, Tree Physiol., 19 (1999) 681–687.

[25] D.E. Pataki, R. Oren, W.K. Smith, Sap flux of co-occurring species in a western subalpine forest during seasonal soil drought, Ecology, 9 (2000) 2557–2566.

[26] A.I. Afangide, I.I. Ekpe, N.H. Okoli, N.T. Egboka, Dynamics of phosphatase enzyme and microbial properties in a degraded ultisol amended with animal manures, J. Clean WAS, 4 (2020) 21–27.

[27] T. Kume, K. Tsuruta, H. Komatsu, T. Kumagai, N. Higashi, Y. Shinohara, K. Otsuki, Effects of sample size on sap flux-based stand-scale transpiration estimates, Tree Physiol., 30 (2010a) 129–138.

[28] A.L. Buck, New equations for computing vapor pressure and enhancement factor, J. Appl. Meteorol., 20 (1981) 1527–1532.

[29] R.O.E. Ulakpa, V.U.D. Okwu, K.E. Chukwu, M.O. Eyankware, Landslide susceptibility modelling in selected states across Se. Nigeria, Environ. Ecosyst. Sci., 4 (2020) 23–27.

[30] J.M. Norman, G. Campbell, An Introduction to Environmental Biophysics, Springer-Verlag, New York, NY, 1998.

[31] D.D. Jiang, F.X. Wan, W.Q. Huang, Slope positions effects on photosynthesis and transpiration characteristics of *Platycladus orientalis* in limestone mountain, China For. Sci. Technol., 6 (2014) 59–63.

[32] T. Kumagai, M. Tateishi, T. Shimizu, K. Otsuki, Transpiration and canopy conductance at two slope positions in a Japanese cedar forest watershed, Agric. For. Meteorol., 148 (2008) 1444–1455.

[33] H.L. Venegas-Quiñones, M. Thomasson, P.A. Garcia-Chevesich, Water scarcity or drought? The cause and solution for the lack of water in Laguna De Aculeo, Water Conserv. Manage., 4 (2020) 42–45.

[34] J. Li, J.F. Huang, X.Z. Wang, L. Zhu, Distribution model of direct solar radiation with high spatial resolution in mountainous areas, Trans. CSAE, 9 (2005) 141–145.

[35] P. Huang, W. Zhao, A.N. Li, Estimation of solar radiation and its spatiotemporal distribution characteristics in the mountainous area of Western Sichuan, Mountain Res., 3 (2017) 420–428.

[36] C.R. Ford, R.M. Hubbard, B.D. Kloeppel, J.M. Vose, A comparison of sap flux-based evapotranspiration estimates with catchment-scale water balance, Agric. For. Meteorol., 145 (2007) 176–185.

[37] L. Jiao, N. Lu, G. Sun, E.J. Ward, B.J. Fu, Biophysical controls on canopy transpiration in a black locust (*Robinia pseudoacacia*) plantation on the semi-arid Loess Plateau, China, Ecohydrology, 9 (2015), 1068–1081.

[38] R.B. Jackson, J.S. Sperry, T.E. Dawson, Root water uptake and transport: using physiological processes in global predictions, Trends Plant Sci., 5 (2000) 482–488.

[39] F. Gu, J. Guo, X. Yao, P. Summers, S. Widijatmoko, P. Hall, An investigation of the current status of recycling spent lithium-ion batteries from consumer electronics in China, J. Cleaner Prod., 161 (2017) 765–780.

[40] F. Gu, J. Guo, W. Zhang, P. Summers, P. Hall, From waste plastics to industrial raw materials: a life cycle assessment of mechanical plastic recycling practice based on a real-world case study, Sci. Total Environ., 601 (2017) 1192–1207.

[41] H. Wang, H. Zhong, G. Bo, Existing forms and changes of nitrogen inside of horizontal subsurface constructed wetlands, Environ. Sci. Pollut. Res., 25 (2018) 771–781.